Available online at www.sciencedirect.com
ScienceDirect
Geochimica et Cosmochimica Acta 73 (2009) 7060–7075
Geochimica et Cosmochimica Acta
www.elsevier.com/locate/gca

Equilibrium $^2H/^1H$ fractionations in organic molecules: I. Experimental calibration of ab initio calculations

Ying Wang [a,*], Alex L. Sessions [a], Robert J. Nielsen [b], William A. Goddard III [b]

[a] Division of Geological and Planetary Sciences, California Institute of Technology, Pasadena, CA, USA
[b] Materials and Process Simulation Center, California Institute of Technology, Pasadena, CA, USA

Received 9 March 2009; accepted in revised form 20 August 2009; available online 23 August 2009

Abstract

Carbon-bound hydrogen in sedimentary organic matter can undergo exchange over geologic timescales, altering its isotopic composition. Studies investigating the natural abundance distribution of ^1H and ^2H in such molecules must account for this exchange, which in turn requires quantitative knowledge regarding the endpoint of exchange, i.e., the equilibrium isotopic fractionation factor (α_{eq}). To date, relevant data have been lacking for molecules larger than methane. Here we describe an experimental method to measure α_{eq} for C-bound H positions adjacent to carbonyl group (H_α) in ketones. H at these positions equilibrates on a timescale of days as a result of keto-enol tautomerism, allowing equilibrium $^2H/^1H$ distributions to be indirectly measured. Molecular vibrations for the same ketone molecules are then computed using Density Functional Theory at the B3LYP/6-311G** level and used to calculate α_{eq} values for H_α. Comparison of experimental and computational results for six different straight and branched ketones yields a temperature-dependent linear calibration curve with slope $= 1.081-0.00376T$ and intercept $= 8.404-0.387T$, where T is temperature in degrees Celsius. Since the dominant systematic error in the calculation (omission of anharmonicity) is of the same size for ketones and C-bound H in most other linear compounds, we propose that this calibration can be applied to analogous calculations for a wide variety of organic molecules with linear carbon skeletons for temperatures below 100 °C. In a companion paper (Wang et al., 2009) we use this new calibration dataset to calculate the temperature-dependent equilibrium isotopic fractionation factors for a range of linear hydrocarbons, alcohols, ethers, ketones, esters and acids.

1. INTRODUCTION

Studies of the natural abundance distribution of the stable isotopes of hydrogen (^1H and ^2H) have facilitated many important scientific findings, ranging from the fundamental basis for isotope effects (Urey et al., 1932; Urey and Rittenberg, 1933) to ecological studies (Estep and Hoering, 1981; Sternberg et al., 1984), paleoclimate reconstructions (Feng and Epstein, 1994), and the origins of petroleum hydrocarbons (Schoell and Whiticar, 1982; Whiticar et al., 1985). More recently, the ability to measure $^2H/^1H$ ratios in individual lipid compounds has enabled many new applications, including the biochemical basis for biosynthetic fractionations (Sessions et al., 1999; Chikaraishi et al., 2004a,b; Zhang and Sachs, 2007; Zhang et al., 2009), apportioning marine versus terrestrial sources of lipids (Chikaraishi and Naraoka, 2003; Li et al., 2009), reconstruction of paleoenvironment (Dawson et al., 2004; Krull et al., 2006), more detailed paleoclimate studies (Pagani et al., 2006; Sachs et al., 2009), the role of H transfer in source rock maturation and petroleum generation processes (Schimmelmann et al., 1999, 2004), and the origin of extremely ^2H-enriched compounds in carbonaceous meteorites (Huang et al., 2005; Gourier et al., 2008).

Hydrogen in organic molecules is affected by a variety of exchange processes that can lead to changes in isotopic

* Corresponding author. Present address: Division of Geological and Planetary Sciences, California Institute of Technology, Mail Code 100-23, 1200 East California Blvd., Pasadena, CA 91125, USA. Tel.: +1 626 200 5850.
E-mail address: ywjojo@gps.caltech.edu (Y. Wang).

0016-7037/$ - see front matter © 2009 Elsevier Ltd. All rights reserved.
doi:10.1016/j.gca.2009.08.019

composition without concomitant changes in molecular structure (Sessions et al., 2004; Schimmelmann et al., 2006). The timescale for such exchange is highly dependent on organic structure, and ranges from seconds for loosely bound H (such as in OH and NH moieties) to millions of years for aliphatic C-bound H at room temperature (Schimmelmann et al., 2006). For studies of individual lipids seeking to reconstruct original biotic or environmental variables, identifying and avoiding such exchange is key (e.g., Andersen et al., 2001; Pedentchouk et al., 2006). For other studies seeking to understand the diagenesis and thermal maturation of sedimentary organic matter (e.g., Schimmelmann et al., 1999; Dawson et al., 2005), the extent and results of exchange are of primary interest. Regardless, in all cases interpreting empirical data requires knowledge of the $^2H/^1H$ distribution expected to result from exchange, i.e., the temperature-dependent equilibrium isotopic fractionation factor (α_{eq}). To cite just one example, observations that sedimentary leaf-wax lipids have very different δ^2H values than co-occurring water have been used to argue that H exchange in *n*-alkanes is very slow (Yang and Huang, 2003). However, such arguments cannot be developed quantitatively unless the resulting equilibrium fractionation is accurately known.

Estimates of equilibrium $^2H/^1H$ fractionations are also relevant to isotopic studies of bulk organic hydrogen, where the contribution from rapidly exchanging H positions must be accounted for (Schimmelmann, 1991). This is typically achieved experimentally by forcing isotopic exchange with water vapors having different $^2H/^1H$ values (Schimmelmann et al., 1999; Sauer et al., 2009). The results of this differential exchange allow the contribution of exchangeable positions to the bulk H pool to be calculated. However, further calculation of the $^2H/^1H$ ratio of non-exchangeable H by mass balance requires knowledge of the equilibrium fractionation factors for exchangeable H positions, which are difficult to obtain experimentally. Only a few estimates for essentially pure substances (e.g., cellulose) are currently available (Schimmelmann, 1991).

To date, there have not been any precise estimates for α_{eq} values in organic compounds larger than methane. Isotope exchange experiments proceed far too slowly for most aliphatic H, with exchange half-lives typically 10^5–10^6 years at 200 °C for aromatic and saturated hydrocarbons without catalysis (reviewed by Sessions et al., 2004). Partial exchange with ^2H_2O is commonly employed to amplify δ^2H shifts (Koepp, 1978; Larcher et al., 1986), but this approach precludes measuring equilibrium fractionations because equilibrium is not reached. Similarly, mineral catalysts and/or high temperatures which speed equilibration often promote side reactions, including rearrangement and oxidation, which confound measurements of pure equilibrium partitioning (Sessions et al., 2004). A few experimental studies have employed isomerase enzymes to catalyze ^3H incorporation into the methyl group of malate (Thomson, 1960) and pyruvate (Meloche et al., 1977) at 35 °C and thus deduced the equilibrium fractionation for $^2H/^1H$ exchange. While useful for some organic species, this approach is not suitable for many molecules that interest organic geochemists, particularly hydrocarbons.

Theoretical calculation of α_{eq}, the alternative approach, was first developed by Urey (1947) and Bigeleisen and Mayer (1947) based on the vibrational energy differences between isotopologues. Although proven to yield accurate results for many isotopic systems, theoretical calculations have not generally been applied to hydrogen isotopes in organic molecules for several reasons. Calculation of the reduced partition function ratio (β factor) requires known molecular vibrational frequencies — generally based on spectroscopic measurements — which are not available for most ^2H-substituted organic molecules relevant to natural systems (Richet et al., 1977; O'Neil, 1986). Computational methods based on molecular simulations, including empirical force fields (Hartshorn and Shiner, 1972) and ab initio modeling (Liu and Tossell, 2005; Hill and Schauble, 2008; Otake et al., 2008) do not require measured vibrational frequencies as inputs, but are accompanied by unknown, and potentially large, systematic errors. This is primarily due to several necessary approximations, including the omission of anharmonicity, rotational corrections, and rotation–vibration coupling terms, which are potentially significant for hydrogen isotopic exchange at room temperature (Richet et al., 1977). Finally, the theory is based on ideal gases, whereas many natural fractionation processes take place in aqueous solution where interactions with solvent molecules could significantly affect internal vibrational modes and contribute to uncertainty (Jancso and Van Hook, 1974).

As a consequence of these difficulties, theoretical estimates for α_{eq} values reported to date are of high precision but poor or unknown accuracy. For example, the overall uncertainty in reported α_{eq} values between aliphatic H and water is typically ±100‰ (Van Hook, 1968; Knyazev et al., 1992; Sessions et al., 2004), almost as large as the fractionation itself. Nevertheless, theoretical calculations provide the only plausible means for estimating α_{eq} values in the huge number of varying organic structures that are encountered in the natural environment. Thus the most efficient way forward is to use empirical and/or experimental data to calibrate a subset of theoretical calculations, which can then be used to efficiently evaluate a much larger range of related structures.

Here we demonstrate one approach to using experimental equilibration data to calibrate theoretical estimates of α_{eq} values. Organic H positions adjacent to carbonyl groups (denoted as H_α) undergo rapid equilibration with water H via keto-enol tautomerism under acid or base catalysis (Appendix A), with exchange half-lives varying from minutes to a few years depending on temperature and pH (Amyes and Richard, 1996; Richard et al., 2001). By equilibrating ketones with waters of varying δ^2H values and measuring the resulting δ^2H values of the ketones at equilibrium, the value of α_{eq} for H_α positions can be derived. Multiple experiments using different molecular structures and different temperatures yield an appropriate calibration dataset for theoretical calculations.

In this paper, we describe the experimental and theoretical methods used to obtain α_{eq} values for exchangeable H in ketones, and report the values of α_{eq} between 0 and 100 °C in seven different structures. We discuss potential

sources of error in the experimental measurements and theoretical calculations, and possible applications of the experimental–theoretical calibration. In a companion paper (Wang et al., 2009), we use the calibration dataset presented here to calculate α_{eq} values for C-bound H in a much wider range of organic molecules with *n*-alkyl skeletons that are relevant to natural environments.

2. NOTATION AND NOMENCLATURE

Throughout this paper, H without superscripts is used to denote hydrogen atoms irrespective of isotopic species, whereas ^{1}H and ^{2}H indicate a specific isotope. Hydrogen isotopic data (^{2}H/^{1}H ratios) are reported as δ^2H values relative to the Vienna Standard Mean Ocean Water (VSMOW) international standard:

$$\delta^2\mathrm{H} = \frac{(^2\mathrm{H}/^1\mathrm{H})_{\mathrm{sample}}}{(^2\mathrm{H}/^1\mathrm{H})_{\mathrm{VSMOW}}} - 1 \quad (1)$$

The permil (‰) symbol used in conjunction with δ^2H values implies a factor of 10^3 which is then omitted from Eq. (1). Differences in isotopic abundance between two species (e.g., organic compound and water) are described by the isotopic fractionation factor (α) and/or isotopic enrichment factor (ε):

$$\alpha_{A,B} = \frac{(^2\mathrm{H}/^1\mathrm{H})_A}{(^2\mathrm{H}/^1\mathrm{H})_B}, \quad \varepsilon_{A,B} = (\alpha_{A,B} - 1)$$

An organic molecule often contains H atoms in different groups which are not chemically equivalent and thus must be characterized by different fractionations (Knyazev et al., 1992; Criss, 1999). When equilibrium has been established between two organic molecules $A\mathrm{H}_m$ and $B\mathrm{H}_n$, each containing q_A and q_B groups of equivalent H atoms, the fractionation factor between the two molecules can be estimated as (Galimov, 1971):

$$\alpha_{eq} = \frac{n\sum_i^{q_A} p_i \beta^i_{A\mathrm{H}_m}}{m\sum_j^{q_B} p_j \beta^j_{B\mathrm{H}_n}} \quad (2)$$

where $\beta^i_{A\mathrm{H}_m}$ and $\beta^j_{B\mathrm{H}_n}$ are the β factor of the *i*th group in $A\mathrm{H}_m$ and the β factor of the *j*th group in $B\mathrm{H}_n$, respectively, and p_i and p_j are the number of equivalent H atoms in the *i*th and *j*th group. Eq. (2) shows that the β factor of the whole molecule takes on the form of the arithmetic mean of the individual beta factors weighted by the number of equivalent H atoms in each group.

Potential for confusion arises because our experiments compare isotopic compositions measured for entire molecules, inferred for certain molecular positions (e.g., all H adjacent to a carbonyl group), and calculated for specific, individual atoms. In the interest of clarity, we adopt the following conventions. (i) All δ^2H values refer to measured isotopic compositions for entire molecules. (ii) Values of α_{eq} (and ε_{eq}) refer to ^{2}H/^{1}H fractionations between organic substrate and water in equilibrium at the specified temperature. The isotope ratio of water is always placed in the denominator, such that a normal isotope effect yielding organic matter depleted in ^{2}H relative to water results in α_{eq} values <1, and ε_{eq} values <0. Note that, when reporting experimental results, α_{eq} refers to all H_α atoms undergoing exchange even if they are not equivalent, such as would be measured in the asymmetric molecule 2-methyl-3-heptanone. In contrast, when reporting theoretical results, α_{eq} refers to the fractionation calculated only for equivalent hydrogen atoms (i.e., the two secondary H_α atoms in 2-methyl-3-heptanone). In each case, the meaning is specified in the text. (iii) In ab initio calculations, H_α positions normally thought to be equivalent (i.e., the three primary H_α atoms on the methyl group of 2-heptanone) yield slightly different fractionations because the molecule is held in a static conformation for the calculations, ignoring the molecular rotations around C–C bonds that occur at ambient temperature. In these cases, we average the fractionations for all nominally equivalent positions to yield a single fractionation factor, which is reported.

The Greek letters α and β are conventionally used to denote the position of carbon atoms relative to a functional group. Unfortunately, they are also used by geochemists to refer to the fractionation factor (α) and reduced partition function ratio (β), respectively. To minimize confusion, we use Greek letters as subscripts to indicate molecular positions, e.g., H_α is the hydrogen atom attached to the first carbon center adjacent to the carbonyl group, H_β is one additional C–C bond further removed, etc. Greek letters not used as subscripts always refer to isotopic fractionations (α_{eq}) or reduced partition function ratios (β).

3. METHODS

3.1. Experimental methods

Seven different volatile ketones were selected as substrates for experimental equilibration with water. Each ketone was fully dissolved in deionized water, sealed in closed vessels with minimal headspace and incubated at constant temperature. At selected time points, samples were removed and the ketone extracted into hexane. The δ^2H values of both ketone and water were then analyzed. The value of α_{eq} between exchangeable H and water at equilibrium can be derived from the slope of a regression between δ^2H values of the ketone and the corresponding waters. Detailed descriptions of each step are presented below.

3.1.1. Materials

Selection of organic substrates is constrained by several factors. Molecules containing a carbonyl functional group are required for rapid equilibration. Given that aldehydes tend to oxidize and esters tend to hydrolyze in basic and acidic conditions, we chose ketones as the substrates for equilibration. To achieve sufficient concentration for isotopic analysis, the aqueous solubility of the substrate must be higher than ~2.5 mM (assuming 100% extraction efficiency), which excludes ketones of carbon number $\geqslant 10$. Small molecules are also preferred because they contain relatively more exchangeable H and thus can produce greater δ^2H shifts during equilibration. However, as size decreases the molecule becomes more hydrophilic and harder to extract. Chromatographic resolution from the solvent peak

also becomes more difficult, which thus excludes ketones of carbon number $\leqslant 4$.

Consequently, we chose 7 ketones ranging from C_6 to C_9, including 2-heptanone (99%), 4-heptanone (98%), 5-nonanone (98%), 2-methyl-3-hexanone (99%), 2,4-dimethyl-3-pentanone (98%), 3,5-dimethyl-4-heptanone (97%) and cyclohexanone (99%) All were obtained from Sigma–Aldrich. They contain primary, secondary and tertiary H_α in linear (straight and branched) ketones and secondary H_α in a cyclic ketone. Fig. 1 gives ball and stick depictions of the optimized structure of each molecule resulting from ab initio modeling (see Section 3.2.2). A large amount of ^2H-enriched water was prepared from distilled water by addition of ^2H_2O (99.5%, Cambridge Isotope Laboratories), and was then mixed with ^2H-depleted water (obtained from a melted Antarctic ice core) at varying volume ratios to produce series of 7–9 waters with evenly spaced δ^2H values between $-286‰$ and $+480‰$. This range brackets the δ^2H values of the unexchanged ketone substrates so that equilibrium can be approached from both directions.

3.1.2. Isotope exchange experiments

Ketones were individually dissolved in each of the 7–9 waters to form 51 different ketone–water solutions. Concentrations of the solutions ranged between 10 and 22 mM, depending on the solubility of the ketone. Solution pH was adjusted to either 12 or 1 with NaOH or HCl, determined at 25 °C using an EC500 pH Meter (Extech).

Experiments were conducted in two stages, with the first designed to estimate exchange rates and the second to accurately measure equilibrium fractionations. In the first stage of experiments, 100 mL aliquots of each solution were sealed in separate glass bottles with rubber septa and incubated in a water bath (Model 202, Napco) at 25, 50 or 70 °C. Aliquots (2 mL) were taken from each bottle at successive time intervals using a glass syringe. Each aliquot

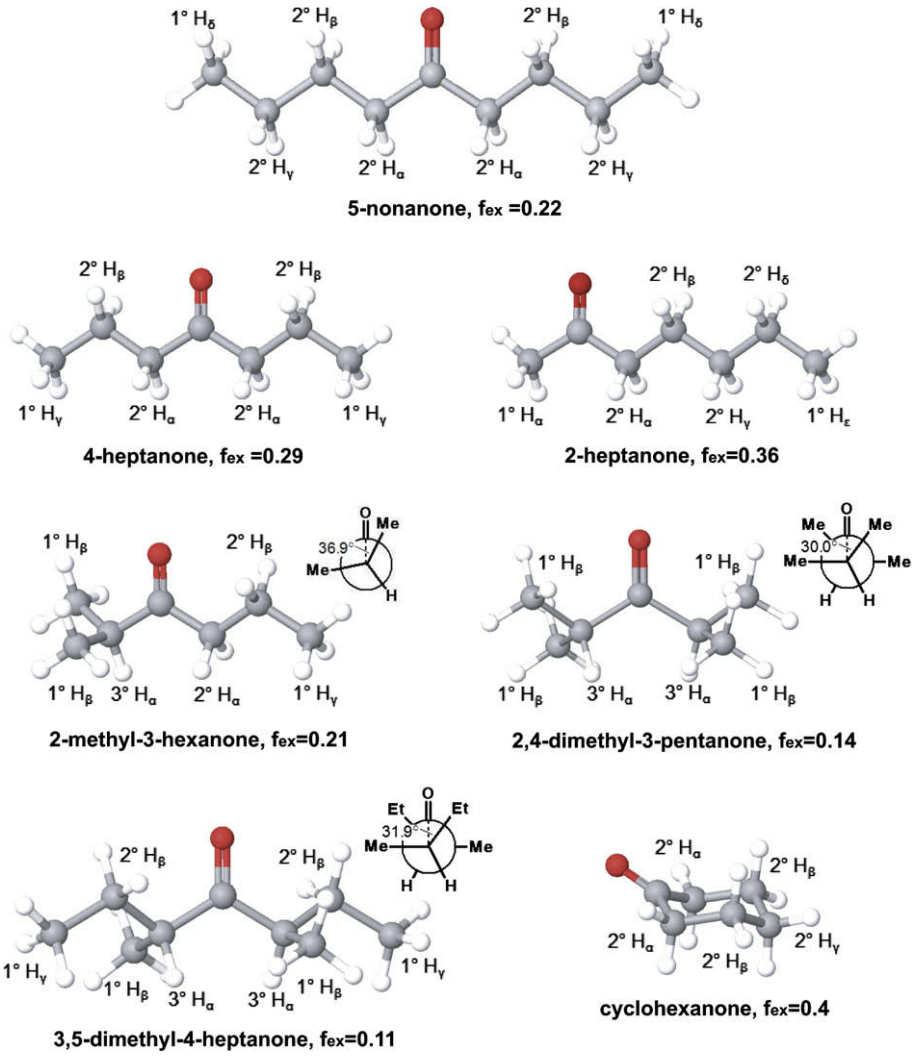

Fig. 1. Optimized geometries of the 7 substrate ketone molecules (● = O, ● = C, ○ = H). H is labeled according to the relative distance from the carbonyl group (subscript Greek letters) and the configuration of the C atom (1° = primary, 2° = secondary, 3° = tertiary). f_{ex} is the fraction of exchangeable H in each molecule, assumed to be exclusively H_α (see Section 3.1.5). The O=C–C_α–C_β dihedral angle is indicated for 2-methyl-3-hexanone, 2,4-dimethyl-3-pentanone and 3,5-dimethyl-4-heptanone.

was immediately extracted by shaking with 6 mL of cold (−18 °C) hexane, with extraction efficiencies between 80% and 95%. The extract was then analyzed without further concentration. From the temporal evolution of substrate δ^2H values and solution pH, exchange rates can be estimated according to the kinetics of second-order reactions (Appendix B). Rate constants were measured for selected combinations of ketone substrate, temperature and pH (see Table 1) so as to estimate the time needed for each of the 7 substrates to reach equilibrium.

Although consecutive sampling of a single bottle yields an exchange profile for the substrate that demonstrates the achievement of equilibrium, repeatedly penetrating the rubber septum over a period of days to weeks can also lead to contamination of the sample with atmospheric water vapor and/or evaporation of the sample. Both effects will bias the measured fractionation factor. This is especially problematic at the highest temperature (70 °C) employed here. Therefore, in the second stage of experiments three 2 mL aliquots of each solution were flame-sealed in glass ampoules so as to exclude any possible evaporation or exchange of water vapor. They were incubated at pH 12.00 in the water bath at 25 ± 0.5 °C, 50 ± 0.8 °C or 70 ± 1.0 °C, respectively. The length of incubation was determined according to rate constants from the first set of experiments, and was always at least 80 exchange half-lives to ensure equilibrium was reached. Following incubation, ampoules were removed from the water bath and quenched in a dry ice/hexane mixture to form ice-water slurry in less than 8 s. Each ampoule was then thawed at room temperature, cracked open, and extracted by shaking with 6 mL cold hexane. The purity of the extracted ketones was checked with a ThermoFinnigan Trace GC equipped with a DB-5 ms column (30 m × 0.25 mm × 0.25 μm) and coupled to a DSQ mass spectrometer (GC/MS). In all cases one peak of greater than 99% purity was observed. The δ^2H value and pH of the water in three randomly selected ampoules were measured before and after the incubation, and no significant change was observed.

3.1.3. Isotopic analysis of ketones

The δ^2H value of each ketone substrate was measured before and after exchange on a ThermoFinnigan Trace GC coupled to a Delta^{plus}XP isotope-ratio mass spectrometer via a pyrolysis reactor (GC/P/IRMS). No Nafion drier was employed. The GC was equipped with a 30 m × 0.32 mm I.D. × 1.0 μm film-thickness EC^{TM}-1 column (Alltech) and a programmable temperature vaporization (PTV) injector that was operated in splitless mode. The pyrolysis tube (Al_2O_3, 0.8 mm I.D. × 305 mm long) was operated at 1440 °C. The flow rate of the carrier gas (He) was 1.4 mL/min. The temperature of the GC oven was initially kept at 40 °C for 4 min, followed by three sequential ramps: 8 °C/min to 100 °C, 20 °C/min to 200 °C and 6 °C/min to 320 °C. Methane reference gas ($\delta^2H = -148‰$) introduced between the downstream end of the GC column and the pyrolysis reactor was used as the internal calibration standard (Wang and Sessions, 2008). Mass-2 and -3 signals were processed using ISODAT NT 2.5 software (ThermoElectron), and data were reported as δ^2H values relative to VSMOW in permil units. The H_3^+ factor was determined daily by measuring the mass 3/2 signal ratio of 10 injections of H_2 reference gas at varying peak height. The value of the H_3^+ factor was very stable at 3.0–3.3 ppm/mV.

Our GC/P/IRMS system exhibits a memory effect of 1–5% between successive peaks separated by 100 s (Wang and Sessions, 2008). If uncorrected, this memory could lead to errors up to 10‰ in the measurements of exchanged ketones, for which δ^2H ranges from −260‰ to +70‰. Moreover, these errors systematically increase with the value of δ^2H and hence will bias the derived fractionation factors. To avoid these problems, a combined calibration-normalization strategy was employed as follows. Three *n*-alkane standards, C_{17} (−142‰), C_{22} (−62.2‰), and C_{27} (−226.5‰), were co-injected with each ketone sample, and a group of four methane reference peaks spaced at 50 s intervals was inserted at 50 s before each of the analyte peaks (Fig. 2a). The last methane peak in each group was used

Table 1
Second-order rate constant and exchange half-life for base-catalyzed H_α exchange. (See Appendix B for calculations).

T (°C)	k_{OH}[a] ($M^{-1}s^{-1}$)	$t_{1/2}$[b] (hours, pH = 12)	$t_{1/2}$[b] (years, pH = 7)	E_a[c] (kJ mol^{-1})
Cyclohexanone				
25	0.0188 (0.0003)	1.0	11.7	45.2 (9.0)
50	0.114 (0.011)	0.2	1.9	
70	0.196 (N/A)	0.1	1.1	
2-Heptanone				
70	0.180 (0.023)	0.1	1.2	
4-Heptanone				
70	0.058 (N/A)	0.3	3.8	
2,4-Dimethyl-3-pentanone				
70	0.016 (0.001)	1.2	14.1	

[a] Second-order rate constant for base-catalyzed H_α substitution, corrected for the number of H_α atoms in each molecule. Uncertainties (1σ) are given in parentheses.
[b] Exchange half-life calculated at pH 12 or 7.
[c] Activation energy calculated according to the Arrhenius relationship.

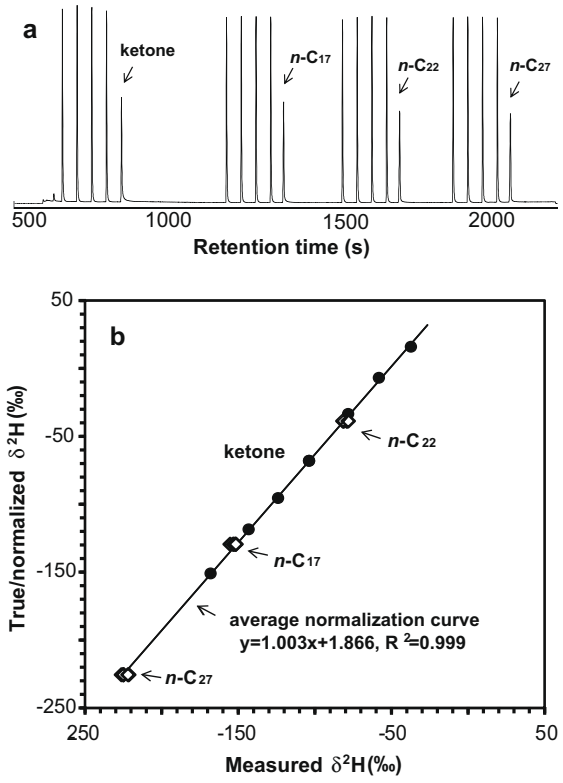

Fig. 2. (a) GC/IRMS chromatogram (*m/z* 2) from a typical analysis of a ketone. Unlabelled peaks are methane reference gas. (b) Normalization curve constructed for analyses of 2-methyl-3-heptanone. The solid circles are data for the 2-methyl-3-heptanone samples exchanged with seven waters of varying δ^2H values. Open diamonds are for the three *n*-alkane standards associated with each analysis and largely overlap.

to calibrate the δ^2H value of the following analyte. Since the peak area (mass-2) was identical (±7%) for each *n*-alkane standard and the ketone analyte, all of them were subject to equivalent memory effects from the preceding methane peaks. Therefore a normalization curve based on the three *n*-alkane standards can be used to correct for memory effects. δ^2H values for the seven exchanged samples of 2-methyl-3-heptanone and for the three *n*-alkane standards in these measurements are plotted in Fig. 2b as an example. Each ketone sample was measured 2–5 times with standard deviation typically between 1‰ and 4‰ (complete δ^2H data are in Electronic Annex Table EA-1). The overall standard deviation for 306 measurements of the *n*-alkane standards was 4‰ for C_{17}, 3‰ for C_{22} and 3‰ for C_{27}.

3.1.4. Isotopic analysis of water

The δ^2H value of water from each sample was analyzed with a DLT-100 liquid–water isotope analyzer (Los Gatos Research, Inc.). A constant volume of 0.65 μL was injected into a heated (70 °C) injection port, and 25 scans were averaged to produce the measured $^2H/^1H$ ratio. A flush cycle of 100 s was adopted between injections to purge residual water vapor from the laser cavity. Six consecutive injections of each sample or standard were measured, with the mean of the last three injections accepted as the final result. Six working standards spanning a similar δ^2H range (−275.2‰ to 457.6‰) as the samples were used for calibration. Since the samples are highly basic (pH 12), we ran the fresh standard every other sample to avoid base precipitates accumulating in the syringe or injection port (Lis et al., 2007). This procedure yielded standard deviations for measured δ^2H values typically between 0.2‰ and 0.4‰.

Because the water and ketone samples were analyzed by independent analytical systems with different standards, it is essential to insure that they are calibrated to the same δ^2H scale to avoid introducing systematic bias into derived fractionation factors. Both the water and organic standards used here were measured by Dr. A. Schimmelmann (Indiana University, Bloomington) using dual-inlet isotope-ratio mass spectrometry. Organic standards were first combusted to water in quartz tubes, and all waters were then reduced to H_2 over hot uranium metal (Schimmelmann and Deniro, 1993). In this way the analyses of both organic and water working standards were calibrated against the same IAEA water standards (VSMOW, SLAP, and GISP).

3.1.5. Calculation of equilibrium fractionation factors

At $^2H/^1H$ exchange equilibrium, the isotopic mass balance for a ketone molecule can be expressed as (Sessions and Hayes, 2005):

$$\delta_T = f_{ex}(\alpha_{eq}\delta_W + \alpha_{eq} - 1) + (1 - f_{ex})\delta_N \quad (3)$$

where δ_T, δ_W and δ_N are the δ^2H values of the total organic molecule, water, and non-exchangeable H, respectively. f_{ex} is the fraction of exchangeable H in the ketone molecule. α_{eq} is the average equilibrium fractionation factor between all exchangeable H in the molecule and water. By regressing δ_T on δ_W, the value of α_{eq} can be obtained from the value of the regression slope divided by f_{ex}, and δ_N can be calculated from the value of the intercept.

Since alkyl H typically exchanges on timescales of millions of years (Koepp, 1978), and keto-enol tautomerism only involves the carbonyl group and C_α position, we assume that only H_α in the ketone molecules is exchangeable during our experiments. The value of f_{ex} thus can be directly determined from the molecular structures (Fig. 1). This assumption can be tested by observing the constancy of δ_N for a ketone incubated at different temperatures.

3.2. Computational methods

3.2.1. Estimation of equilibrium fractionation factors

$^2H/^1H$ exchange between two compounds, AH and BH, can be described by the reaction:

$$A^1H + B^2H = A^2H + B^1H$$

For the exchange of a single H atom, the value of α_{eq} is equal to that of the equilibrium constant, K_{eq}, which can be expressed as the ratio of the total partition function ratios between the compounds in equilibrium:

$$\alpha_{eq} = K_{eq} = \frac{Q(A^2H)/Q(A^1H)}{Q(B^2H)/Q(B^1H)} \quad (4)$$

where Q is the total partition function of the indicated species. It was first shown by Urey (1947) and Bigeleisen and Mayer (1947) that the total partition function ratio can be approximately described by molecular vibrations in the form of the reduced partition function ratio, known as the β factor. Therefore α_{eq} can be written as

$$\alpha_{eq} = \frac{\beta(A\mathrm{H})}{\beta(B\mathrm{H})} \tag{5}$$

The value of β, under the Born–Oppenheimer and Harmonic Oscillator approximations and the Redlich–Teller Product Rule, is calculated as:

$$\beta = \prod_{i}^{3N-6} \frac{u_{2i}}{u_{1i}} \cdot \frac{exp(-u_{2i}/2)}{exp(-u_{1i}/2)} \cdot \frac{(1 - exp(-u_{1i}))}{(1 - exp(-u_{2i}))} \tag{6}$$

in which

$$u_i = \frac{h\nu_i}{k_B T} \tag{7}$$

$3N$-6 is the number of normal modes for nonlinear molecules, ν_i is the vibrational frequency of the ith normal-mode, h is Planck's constant, k_B is Boltzmann's constant, and T is temperature in Kelvin. Symmetry numbers that would otherwise clutter the expression of β are omitted because they cancel in the calculation of α_{eq} (Eq. (5)).

3.2.2. Ab initio modeling

Vibrational frequencies of each organic molecule were calculated using the Density Functional Theory (DFT) approximation (Greeley et al., 1994) to quantum mechanics, performed using Jaguar 7.0 (Schrödinger Inc.). In particular we use the B3LYP flavor of DFT (Lee et al., 1988; Becke, 1993) which has been established to provide systematically accurate energetics, structures, and vibrational frequencies for a wide range of organic molecules (Xu et al., 2005). The B3LYP calculations used the 6-311G** basis set, a triple split-valence basis set with polarization functions on all atoms. The solvation effect for organic molecules was simulated using the Poisson–Boltzmann continuum solvation model (Tannor et al., 1994) as implemented in Jaguar. These computations were carried out using the following procedures.

Starting with a best-guess molecular geometry, an optimized geometry was first calculated in the gaseous phase and then re-optimized in the aqueous phase. For molecules with branched carbon chains, we first performed a conformation scan of internal torsion with 15° increments (see Section 4.2.1). The conformation with the minimum energy on the potential surface was then used as the initial guess for geometry optimization. The convergence criterion for the DFT electronic structure calculations was 5×10^{-5} hartree for energy and 5×10^{-6} hartree/Bohr for root-mean-squared (RMS) change in density matrix. The convergence criterion for optimization of the structures was 5×10^{-5} hartree for energy. The convergence criteria for optimization in solution are three times larger than in the gas phase.

The Hessian matrix (second derivatives with respect to atom positions) was calculated numerically for the optimized geometry. The same Hessian matrix was then used to calculate vibrational frequencies for isotopologues. No scaling factor was applied. Using these frequencies, the β factor was calculated (Eq. (6)) with respect to ^{2}H-substitution at individual H_α positions in an aqueous environment over the range of 0–100 °C.

Calculation of the β factor for water was first performed on isolated molecules, i.e., as an ideal gas, following the same method (B3LYP/6-311G**) as above. The solvation effect, however, was not treated in the same way. On one hand, implicit solvation methods cannot account for the external modes in condensed phase which are more important for water molecules that are affected by hydrogen bonding than for large organic molecules with hydrophobic chains. On the other hand, explicit hydration models are limited by the number of water molecules and the configuration of the water cluster, and are thus inadequate to describe the bulk liquid water (Felipe et al., 2003). To avoid such issues, we therefore chose to multiply the ideal-gas β factor by the experimentally measured liquid–vapor fractionation factor (Horita and Wesolowski, 1994) to obtain β factors for liquid water. This approach is presumably more accurate than calculations based on solvation models of liquid water. The value of α_{eq} was then calculated as the ratio of β factors between the organic molecule in aqueous phase and liquid water.

4. RESULTS AND DISCUSSION

4.1. Isotope exchange experiments

4.1.1. Exchange kinetics

In time-series experiments, ^{2}H/^{1}H exchange profiles were measured for all substrates at 70 °C, pH 12. They were also measured for cyclohexanone at 25 and 50 °C, pH 12; for cyclohexanone at 25 °C, pH 1; and for 2-heptanone at 70 °C, pH 1.2. Exchange rates, half-lives ($t_{1/2}$) and activation energy (E_a) were estimated (Appendix B). The results are summarized in Table 1.

Selected data for cyclohexanone are plotted in Fig. 3 as an example (data for other ketones are shown in Fig. EA-1). The δ^2H values of the ketone changed systematically with time, clearly recording the progress of ^{2}H/^{1}H exchange between ketone and water. At a specific temperature and pH, all incubations reached equilibrium simultaneously, as indicated by stable δ^2H values with time. At 25 °C and pH 12, equilibrium was achieved within four days ($\sim 5 \times 10^3$ min). Exchange was faster at 50 °C and pH 12, with equilibrium reached in less than 12 h ($\sim 5 \times 10^2$ min). In contrast, exchange at 25 °C and pH 1 was much slower, where $t_{1/2}$ was estimated to be 6 days and equilibrium was not reached within two months. The attainment of isotopic equilibrium under acid catalysis was confirmed for 2-heptanone (Fig. EA-1). In this case, measured ketone δD values at equilibrium and the calculated fractionation factor are equivalent to those measured under basic conditions. Since apparent exchange rate is proportional to the concentration of H^+ or OH^- (Appendix A), our data indicate that OH^- is much more efficient than H^+ at catalyzing H_α substitution. Basic conditions (pH 12) were thus employed in most experiments.

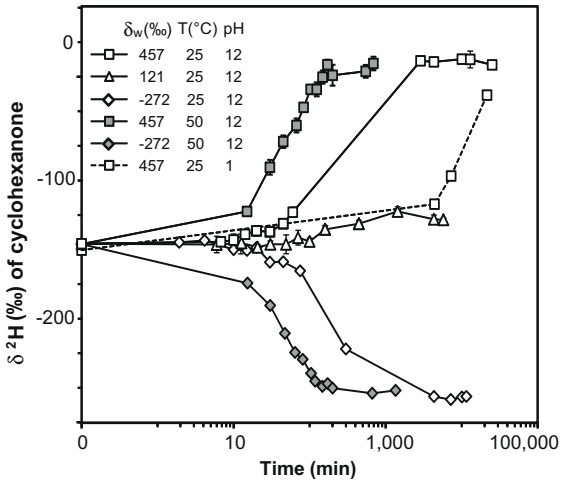

Fig. 3. Cyclohexanone δ^2H values over time during incubations with waters of varying δ^2H values, temperature and pH (shown in legend). Note the logarithmic *x*-axis. Error bars represent standard deviations from 3 to 5 measurements of the same sample and are generally smaller than the symbols.

At 70 °C, the exchange rate for secondary H_α in 4-heptanone is faster than for tertiary H_α in 2,4-dimethyl-3-pentanone, while the rate for primary H_α in 2-heptanone, estimated from the results of 2-heptanone and 4-heptanone, is even faster. The decrease of exchange rate with increasing alkyl substitution on C_α is probably related to steric hindrance of the alkyl group(s) on the H_α position. The activation energy for base-catalyzed H_α exchange is calculated to be 45.2 ± 9.0 kJ mol^{-1} for cyclohexanone. Approximate rate constants for linear ketones at 50 and 25 °C can be estimated by assuming the same activation energy as for cyclohexanone.

When extrapolated to neutral pH, $t_{1/2}$ is estimated to be several years for temperatures comparable to those of diagenesis (Table 1). Exchange in natural environments is probably much faster, because of the presence of enzymes (Richard et al., 2001) and mineral surfaces (Alexander et al., 1982) that are potent catalysts. H_α substitution in carbonyl compounds other than ketones, e.g., carboxylic acids and their derivatives [R(C=O)X, where X = OH/O$^-$/OR/SR/NH$_2$...], also proceeds via keto-enol tautomerism and facilitates many diagenetic transformation reactions such as the racemization of amino acids. At neutral pH, H_α in oxy- and thiol-esters exchanges on timescales of 10^1–10^2 years (Amyes and Richard, 1996), comparable to ketones, while H_α in amides and the anions of carboxylic acids exchanges slowly, with $t_{1/2}$ on the order of 10^7 years. Under conditions typical of certain lab procedures, e.g., the demineralization of sediments to isolate organic matter, where organic compounds are exposed to strong acids and elevated temperatures, H_α exchange will be considerably faster. However, the impact of this exchange on isotopic analysis should — in most cases — be minimal due to the low fraction of exchangeable H in most lipids.

4.1.2. Experimental measurements of equilibrium fractionation factors

During the second stage of $^2H/^1H$ exchange experiments, incubations were carried out with all substrates at pH 12 for 7 days, 22 days and 85 days at 70, 50 and 25 °C, respectively, more than 80 times longer than the estimated $t_{1/2}$ at each temperature. Equilibrium fractionation factors for H_α are derived from the regression slope between δ^2H values of the ketone and water at equilibrium (Eq. (3)). This yields a single value of α_{eq} that applies to all exchanging H_α positions, regardless of whether they are equivalent. R^2 values for these regressions are all greater than 0.99. Data for 2,4-dimethyl-3-pentanone are plotted as an example in Fig. 4. Complete δ^2H data for incubated ketones and water are presented in Electronic Annex (EA) Table EA-1.

Derived values of the equilibrium fractionation (expressed as the isotopic enrichment factor, ε_{eq}) for exchanging H_α positions of the ketone substrates are summarized in Table 2 and Fig. 5. The uncertainty in ε_{eq} values, generally between 10‰ and 20‰, is estimated from the standard deviation of the regression. The relatively large uncertainty for 5-nonanone at 70 °C is due to the loss of two samples, while that for 2-heptanone at 25 and 50 °C is probably related to variation in analyte abundance during GC/P/IRMS analysis. The values of δ_N in each ketone are statistically identical at different temperatures, confirming our assumption that only H_α is undergoing appreciable exchange during the incubations.

The two ketones that contain only tertiary H_α atoms, 3,5-dimethyl-4-heptanone and 2,4-dimethly-3-pentanone, yield similar ε_{eq} values ranging between +27‰ and −32‰ and negative temperature dependence with a crossover of $\varepsilon_{eq} = 0$ at about 55 °C (Fig. 5). Ketones containing only secondary H_α atoms, 4-heptanone and 5-nonanone, have similar ε_{eq} values between −130‰ and −112‰ with little temperature variation. The value of ε_{eq} for 2-methyl-3-hexanone, a

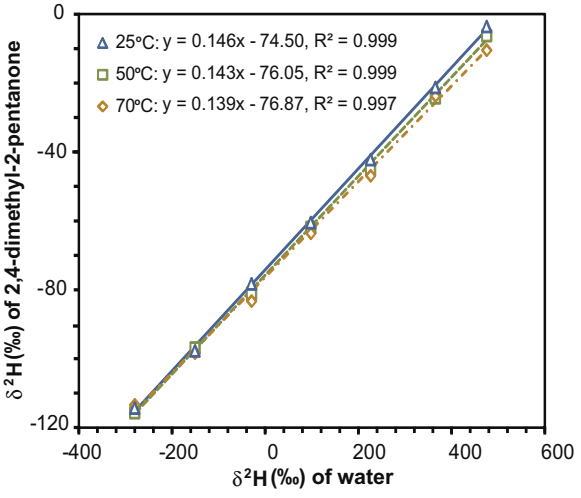

Fig. 4. Regression of δ^2H values for 2,4-dimethyl-3-pentanone and water in equilibrium at pH 12 and 25 °C (solid line), 50 °C (dashed line) and 70 °C (dot-and-dash line). Analytical uncertainties for each data point are smaller than the symbols.

Table 2
Experimental isotopic enrichment factors (ε_{eq}) for H_α and δ^2H values for non-exchangeable H (δ_N) in the seven ketones.

Ketone substrate	25 °C		50 °C		70 °C	
	ε_{eq} (‰)	δ_N (‰)	ε_{eq} (‰)	δ_N (‰)	ε_{eq} (‰)	δ_N (‰)
2,4-Dimethyl-3-pentanone	27 (11)	−91 (2)	4 (12)	−89 (2)	−25 (20)	−85 (4)
3,5-Dimethyl-4-heptanone	8 (16)	−54 (2)	−18 (20)	−45 (3)	−32 (17)	−47 (5)
2-Methyl-3-hexanone	−81 (6)	−111 (2)	−65 (8)	−109 (2)	−90 (17)	−109 (5)
4-Heptanone	−130 (22)	−69 (9)	−129 (17)	−55(7)	−112 (21)	−79 (9)
5-Nonanone	−122 (12)	−74 (3)	−112 (18)	−76 (5)	−128 (29)	−80 (9)
2-Heptanone	−152 (30)	−58 (17)	−145 (25)	−42 (14)	−140 (19)	−39 (11)
Cyclohexanone	−161 (11)	−171 (8)	−155 (10)	−182 (7)	−138 (10)	−198 (7)

Uncertainties (1σ) are given in parentheses. They are propagated from the standard error of the regression slope and intercept.

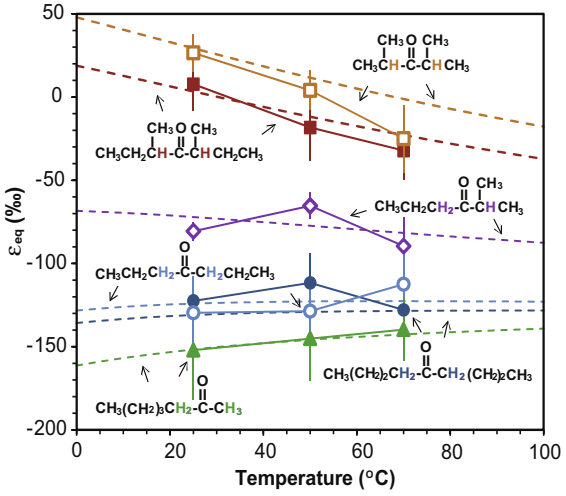

Fig. 5. Equilibrium isotopic enrichment factors (ε_{eq}) for H_α in linear ketones as a function of temperature. Symbols represent experimental results measured at 25, 50 and 70 °C with error bars of $\pm 1\sigma$. Dashed lines represent theoretical results from 0 to 100 °C for the same molecules (see Section 4.2.2). Data represent the weighted average for all H_α atoms in each ketone.

molecule containing one tertiary and two secondary H_α atoms, agrees well with the weighted average of tertiary H_α and secondary H_α. ε_{eq} for primary H_α is difficult to measure directly because the appropriate substrate — acetone — is both highly soluble in water and volatile. Instead, it was calculated by mass balance from ε_{eq} values for 2-heptanone and for secondary H_α in 4-heptanone and 5-nonanone. The result is −172‰ at 25 °C, −167‰ at 50 °C and −148‰ at 70 °C. H_α in cyclohexanone has ε_{eq} values (Table 2) between those for primary and secondary H_α in linear ketones.

The value of ε_{eq} for H_α increases substantially with more alkyl substituents attached to C_α. This is likely due to the electron-donating effect of alkyl groups, with methyl groups being the strongest donor. It acts to enhance the electron density of the C_α–H_α bond and thus increases bond strength. As an example, the calculated force constants for the C_α–H_α stretching mode are 1.01, 1.39, 2.31 and 2.42 mDyne/Å for acetone, 4-heptanone, 3,5-dimethyl-4-pentanone and 2,4-dimethyl-3-pentanone, respectively. Since heavier isotopes partition preferentially into stiffer bonds (Bigeleisen and Mayer, 1947), the value of ε_{eq} is thus larger for an H bonded to C with more alkyl substitution. Hartshorn and Shiner (1972) fitted force fields to published vibrational frequencies for a series of small organic molecules (<C_3) and their ^2H-isotopologues, and then used those force fields to calculate α_{eq} relative to acetylene H at 25 °C. They found that the successive replacement of H by C on a CH_3 group will result in a α_{eq} ratio of about 1.10 between the two molecules. Our results give a ratio of 1.055 between secondary H_α and primary H_α and 1.174 between tertiary H_α and secondary H_α, generally consistent with their results. In addition, their calculations revealed that α_{eq} for secondary H in cyclic hydrocarbons is lower than that in linear hydrocarbons by a ratio of 0.93, also consistent with the corresponding ratio of 0.959 in our study. Thomson (1960) and Meloche et al. (1977) used isomerase enzymes to catalyze ^3H incorporation at 35 °C and thereby deduced the value of α_{eq} to be −160‰ for the primary H_α in pyruvate and −70‰ for the secondary H_α in malate, both comparable to our results.

Another noteworthy feature is that equilibrium $^2H/^1H$ fractionation is mainly affected by atoms directly bound to the same C atom, and is only slightly affected by more remote structures. This "cutoff effect" has been demonstrated in several theoretical studies of isotope effects in organic molecules (Stern and Wolfsberg, 1966a,b; Hartshorn and Shiner, 1972), and is discussed further in Section 4.4.2.

4.2. Theoretical calculations

4.2.1. Optimized molecular geometries

Optimized geometries for the 7 ketone substrates in the gas phase are shown in Fig. 1. Selected bond lengths and bond angles are given in Table EA-2. For ketones with branched carbon chains, including 2-methyl-3-hexanone, 2,4-dimethyl-3-pentanone and 3,5-dimethyl-4-heptanone, a conformation scan of internal torsion about the O=C–C_α–C_β dihedral shows that they are most stable when one alkyl branch is at 30–37° to the carbonyl group (Fig. 6 and inserts of Fig. 1). Similar stable conformations were found by Langley et al. (2001) for 3-methyl-2-butanone and 2,4-dimethyl-3-pentanone using B3LYP/6-31G* and molecular mechanics (MM3 and MM4) methods.

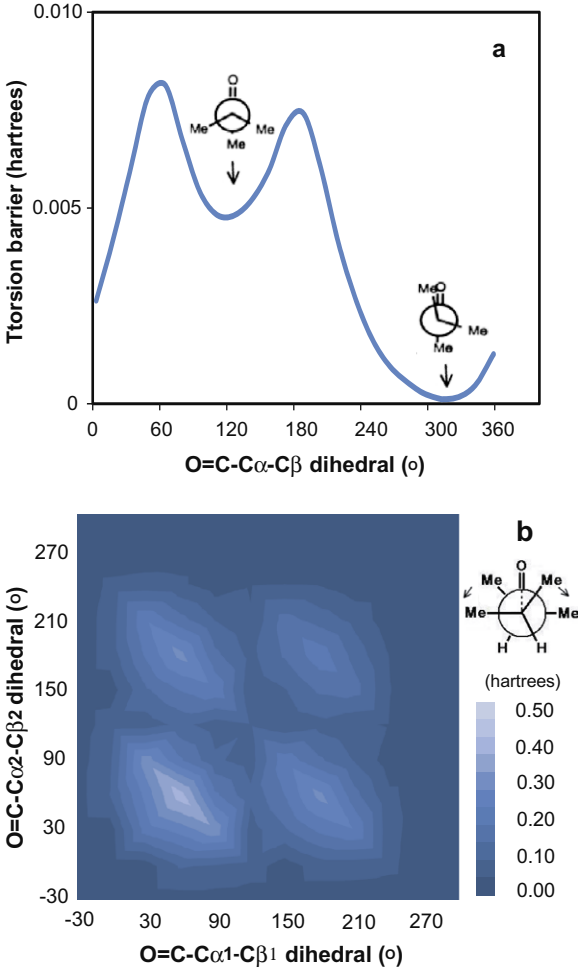

Fig. 6. Molecular potential curve of the internal torsion about the O=C–C_α–C_β dihedral with 15° increments for (a) 2-methyl-3-hexanone and (b) 2,4-dimethyl-3-pentanone.

4.2.2. Theoretical estimates of equilibrium fractionation factors

Values of the β factor were calculated from 0 to 100 °C for each H_α position in the incubated ketone molecules and for water (complete β factor values are in Table EA-3 and -4). For each ketone molecule, the reported value of ε_{eq} is the weighted average for all individual H_α positions.

Calculated values of ε_{eq} for the six linear ketone substrates are plotted together with the corresponding experimental results in Fig. 5. They agree well in both magnitude and temperature dependence. As for the experimental results, calculated ε_{eq} values for H_α in structurally similar molecules are consistent. At 25 °C, the standard deviation (σ) of ε_{eq} values for secondary H_α in 4-heptanone, 5-nonanone, 2-heptanone and 2-methyl-3-hexanone is 3‰. Tertiary H_α in 2,4-dimethly-3-pentanone and 2-methyl-3-hexanone has consistent ε_{eq} values ($\sigma = 2$‰) that are 20–30‰ higher than the tertiary H_α in 3,5-dimethly-4-heptanone. This is consistent with the experimental results and is likely due to the stronger electron-donating ability of methyl groups than that of other alkyl groups (the C_α at C-2 in 2,4-dimethly-3-pentanone and 2-methyl-3-hexanone has two methyl branches, whereas the C_α at C-3 in 3,5-dimethly-4-heptanone has only one methyl branch).

In contrast, theoretical ε_{eq} values for cyclohexanone (based on unscaled frequencies) are ~60‰ higher than the experimental results. It thus seems that while our computational approach does an excellent job of reproducing experimental data for linear ketones, that approach does not yield accurate results for cyclic compounds (see Section 4.4.3. for more discussion).

4.3. Comparison of experimental and theoretical equilibrium fractionations

Experimental versus theoretical isotopic enrichment factors (ε_{eq}) for H_α in the 6 linear ketones are plotted in Fig. 7. In general, experiment and theory agree quite well. As temperature increases, there is a general trend towards slightly lower slope (0.982 ± 0.035 at 25 °C, 0.904 ± 0.072 at 50 °C and 0.811 ± 0.038 at 70 °C), i.e., the calibration curve is temperature-dependent. The trend is driven primarily by variations in tertiary H_α positions, and presumably indicates some aspect of the experiments that was not fully captured by the ab initio calculations (see discussion in Section 4.4.2).

We therefore adopt a temperature-dependent calibration curve by fitting the regression slope and intercept, respectively, to temperature (Fig. 8). This approach gives slope $= 1.081–0.00376T$ and intercept $= 8.404–0.387T$, where T is temperature in degrees Celsius. This temperature-dependent calibration scheme is then used in a companion paper (Wang et al., 2009) to correct the calculated isotope enrichment factor for other organic molecules. As a simpler alternative, and considering the 10–20‰ experimental errors, one could use a temperature-averaged calibration curve (slope $= 0.914 \pm 0.032$, intercept $= -8.86 \pm 3.22$) derived from all 18 data points in Fig. 7. The two ap-

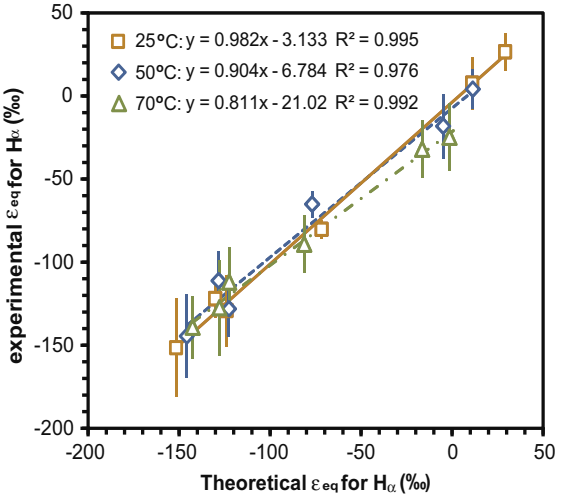

Fig. 7. Regressions between experimental and theoretical ε_{eq} values for H_α in six linear ketones at 25 °C (solid), 50 °C (dash) and 70 °C (dot-and-dash), respectively. Error bars represent $\pm 1\sigma$ in experimental ε_{eq} values.

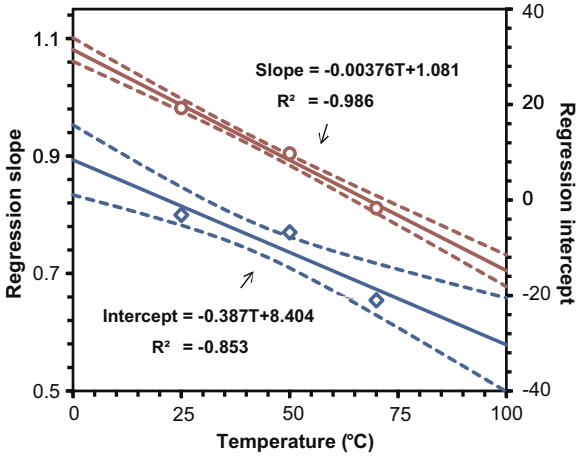

Fig. 8. Regression of the calibration slope (circles) and intercept (diamonds) against temperature. Dashed lines indicate $\pm 1\sigma$ for the estimated slope or intercept at any temperature between 0 and 100 °C.

proaches yield calibrated isotopic enrichment factors that differ by less than 12‰ between 0 and 100 °C.

4.4. Sources of error

Uncertainty in the calibration represented by Fig. 7, and in its application to other molecules, encompasses potential systematic errors in both experimental measurements and ab initio calculations. Here we attempt to describe and quantify those uncertainties.

4.4.1. Experimental uncertainties

For the experimental dataset, the most likely potential sources of error are (i) failure to achieve true equilibrium, (ii) fractionations arising during sample extraction and handling, and (iii) systematic biases in measured δ^2H values. The attainment of equilibrium in our samples is demonstrable in two ways. First, equilibrium was approached from both directions by using waters of varying $^2H/^1H$ ratios. While it is true that partial equilibration of samples could still lead to a linear relationship between δ^2H values for the substrate and water, this would yield consistent fractionations for different molecules only if they exchanged at exactly the same rate, which is demonstrably untrue. Second, isotopic exchange of 2-heptanone under both acidic and basic conditions (Fig. EA-1) — which catalyze very different exchange rates — yielded indistinguishable fractionations, strongly supporting the attainment of equilibrium.

To evaluate potential isotopic fractionations of ketones during sample extraction and handling, we conducted control experiments in which cyclohexanone, 4-heptanone and 2-heptanone were each dissolved in neutral deionized water at 25 °C and then extracted without any equilibration. The resultant δ^2H values of the ketones were indistinguishable from those measured for the pure substances.

Because the measured δ^2H values for waters and ketones cover a large range of isotopic compositions, there is also a possibility for systematic biases in their measured values to arise. Such an effect is commonly referred to as 'scale compression', and is known to vary between individual mass spectrometers (Coplen, 1988). Our extensive use of multiple organic and water working standards which span the range of measured δ^2H values and are both calibrated to the IAEA SMOW/SLAP scale, should largely mitigate such effects. Although minor artifacts of scale compression may still remain, they are likely <10‰. Thus we believe that systematic errors in the experimental data are likely to be small, and the uncertainties stated in Table 2 (which are based solely on the statistics of linear regression) provide an adequate estimate of both precision and accuracy for this dataset.

4.4.2. Uncertainties in ab initio calculations

Approximations adopted in the calculation of β factors, primarily the omission of anharmonicity, rotational correction, and rotation–vibration coupling, are generally expected to result in significant systematic errors for hydrogen isotopic fractionations. The excellent agreement between theoretical and experimental ε_{eq} values for linear ketones was thus unexpected. An important point is that only the ratios of partition functions and β factors enter into the calculation of α_{eq} and ε_{eq}. Since the same calculation methods (except for the solvation model) were applied to both water and ketone molecules, systematic errors in their β factors are expected to be positively correlated and tend to cancel, as pointed out by Hartshorn and Shiner (1972) and Liu and Tossell (2005).

To help pinpoint the importance of various error sources, we compared our calculated β factor for water to the result of Richet et al. (1977), who calculated various small molecules by taking into account the effects of anharmonicity, rotational correction and rotation–vibration coupling. At 30 °C, their β factor for an isolated water molecule is 11.064, smaller than our result (12.516) by a factor of 0.884. By reproducing their calculation using the molecular constants provided in the paper, we find that this discrepancy is primarily due to the omission of the anharmonic correction to zero point energy (ZPE) in our calculation, which alone contributes a factor of 0.888. This term arises from the anharmonicity of various normal modes and their couplings at the ZPE level. Adding the rotational correction introduces a factor of 0.995. The anharmonic effect on excited vibrational states and the rotation–vibration coupling lead to factors of 1.00009 and 0.99998, respectively, and thus can be safely ignored. Note that the solvation effect for water is treated by multiplying the β factor for a gaseous molecule with the experimental liquid–gas fractionation factor, which is presumably free of systematic error. The overall uncertainty in the β factor of liquid water is therefore dominated by the omission of anharmonity at the ZPE level.

The significance of the above errors to the β factor for ketones can only be evaluated qualitatively, because the relevant molecular constants needed for quantitative calculations are unknown. The ketones studied here are large polyatomic molecules, and their moments of inertia are large enough that rotational corrections are negligible at or above room temperature (Bigeleisen and Mayer, 1947).

The effect of rotation–vibration coupling is difficult to evaluate but unlikely to be orders of magnitude larger for the ketone than for water molecules.

Errors associated with use of the PCM solvation model can be assessed as follows. The measured vapor pressure isotope effect (VPIE) for hydrocarbons is small (~4‰) at 24 °C (Wang and Huang, 2001). We also calculated VPIE over 0–100 °C for the ketones used in our calibration, with the results generally between 0‰ and 10‰. Thus correction for the solvation effect is at most ~10‰, and systematic errors associated with the specific PCM model are likely to be smaller than that. We also tested the effects of using explicit hydration with three, four and five water molecules in our calculations. The resulting fractionation factors for the six linear ketones were then regressed against the experimental results, which give regression slopes around 1.1 and intercepts between 10‰ and 40‰ (summarized in Table EA-5), with even larger temperature variability than that using implicit solvation model. Although explicit H-bonding was shown to have significant effect on hydrogen equilibrium fractionation factors in the H_4SiO_4–H_2O system (Felipe et al., 2003), it is apparently much less important for C-bound H that interacts weakly with water, compared to O-bound H.

The size of anharmonic effects on the value of β factors for ketones can be qualitatively evaluated by examining the 'frequency scaling factor'. For a specific ab initio method, the scaling factor is obtained by calibrating the calculated vibrational frequencies against corresponding experimental frequencies to correct the former for anharmonic effects. The precision and accuracy of the scaling factor thus depend on the size and diversity of the calibration dataset. However, applying scaled ab initio frequencies to calculate β factors using the Bigeleisen–Mayer–Urey equation (Eq. (6)), which adopts the Harmonic Oscillator approximation, will overestimate the anharmonic correction to ZPE (Scott and Radom, 1996; Otake et al., 2008) and will not correctly account for the anharmonic effect on excited vibrational states. Thus applying these scaling factors alone cannot produce accurate β factors (see Table EA-5). Nevertheless, they can be used to evaluate the relative significance of anharmonicity between various species. We therefore applied the recommended scaling factor for B3LYP/6-311G** (0.967, Computational Chemistry Comparison and Benchmark DataBase (CCCBDB), NIST) and recalculated β factors based on the scaled frequencies. Results are plotted in Fig. 9 as the ratio of β factors calculated using scaled (β_s) and unscaled (β_u) frequencies.

Fig. 9 shows that anharmonicity uniformly lowers the value of β factor to similar extents (β_s/β_u ~0.9) for both water and ketones, which implies that errors due to the omission of anharmonicity will largely cancel when β_u is used to calculate α_{eq}, consistent with the excellent agreement between experiment and theory for linear ketones. The β_s/β_u ratios for the ketones are slightly below that for water. Therefore, accounting for anharmonicity will lower the β factor for ketones more than that for water, and thereby decrease the fractionation factor. This is consistent with the fact that the experimentally determined fractionation factors are generally more negative than the calculated fractionation factors (calibration intercepts <0). Moreover, the β_s/β_u ratio progressively decreases from primary to secondary and tertiary H_α, such that accounting for anharmonicity will lower the β factor for tertiary H_α (with positive ε_{eq} values) more than that for primary H_α (with the most negative ε_{eq} values), leading to calibration slopes <1.

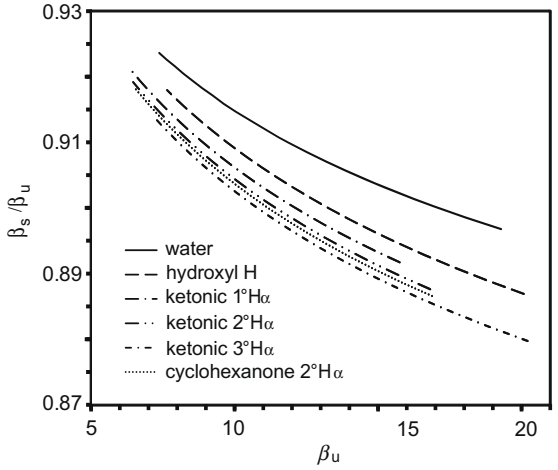

Fig. 9. The ratio between β factors calculated using scaled frequencies (β_s) and those using unscaled frequencies (β_u) over 0–100 °C. The same type of H, i.e., primary (1°), secondary (2°), tertiary (3°) or hydroxyl H, in various organic molecules gives virtually the same results.

Anharmonicity is also likely responsible for the temperature dependence of our calibration curve, because its effect gradually increases with temperature while the harmonic term rapidly decreases. Otake et al. (2008) showed that the relative decrease in β factors due to anharmonicity is larger at higher temperature and for molecules of larger size. Therefore the cancelation of errors between ketone and water will vary slightly with temperature, and potentially give rise to the temperature dependence of the experimental–theoretical calibration. As shown in Fig. 7, lowering of the regression slope is primarily due to the fast decrease in ε_{eq} values of tertiary H_α, for which the mechanism is currently unclear.

Another mechanism possibly underlying the temperature variability is conformational changes with temperature. The ketones are large floppy molecules for which long-range internal torsion along the carbon chain can exist at ambient temperatures. Therefore, a single stable conformation might be inadequate to describe the real molecule, especially at higher temperatures. Using 2,4-dimethyl-3-pentanone (the ketone showing the largest temperature variation in ε_{eq} values) as an example, we calculated its entire torsional potential around the O=C–C–C dihedral. The value of ε_{eq} was then calculated for the optimized geometry at each local minimum and weighted according to the Boltzmann distribution to generate a conformation-averaged fractionation factor. The result is indistinguishable from that based on a single geometry at the global minimum across the range of 0–100 °C. This observation is consistent with the "cutoff" effect found in previous studies (Stern and Wolfsberg, 1966a,b; Hartshorn and Shiner,

1972), wherein structures beyond the γ position from the substituted atom can be largely ignored in the calculation of isotopic fractionation. It is also buttressed by the frequency data, which show that the value of the β factor is mainly controlled by the isotopic frequency shifts in the stretching and bending modes that directly involve the substituted C–H bond, whereas frequency shifts for the torsional modes are more than 100 times smaller.

In conclusion, uncertainties in the ab initio calculation are likely dominated by anharmonic effects, based on their capacity to explain most discrepancies between theory and experiment. Variation in the size of anharmonic effects with changing temperature and H position probably leads to the observed temperature-dependence of the calibration curve, which cannot be corrected by simply applying the scaling factor (see Table EA-5). Quantitative calculation of anharmonicity requires computing a wide range of the entire potential surface (Young, 2001; Otake et al., 2008) which would be prohibitively time-consuming for the large organic molecules we deal with.

4.4.3. Limitations in applying the calibration to other molecules

To estimate the error that might arise from applying our calibration to molecules other than ketones, we first analyzed variations in the value of the scaling factor. To do so, we calculated the scaling factor using frequency data from the CCCBDB database for individual compound classes, including linear alkanes, alkenes, ketones, aldehydes, esters, ethers and alcohols. Their scaling factors are very consistent at 0.967 ± 0.002. Then we applied this scaling factor to calculate the β_s/β_u ratio for C-bound H in these compounds. The results are virtually identical to those in ketones for analogous positions (primary, secondary, tertiary), indicating that the relative size of anharmonicity is consistent for the three types of H positions in linear molecules. Therefore our calibration curve based on ketones should be widely applicable to other *n*-alkyl compounds. When the ± 0.002 uncertainty in scaling factor is propagated into the calculation of ε_{eq}, the results vary by ±4–8‰ (1σ). We take this range as a conservative estimate of systematic biases arising from the application of our calibration curve to other linear molecules. It is only about one-third as large as uncertainties in the experimental calibration dataset.

We further note that the β_s/β_u ratios for hydroxyl H in alcohols and carboxylic acids are slightly higher than those for C-bound H (Fig. 9). As a result, applying the same calibration tends to systematically underestimate ε_{eq} for hydroxyl H by 6–10‰. Also, β_s/β_u ratios for H_α in cyclohexanone are virtually the same as those for linear ketones (Fig. 9), implying that the significant offsets between experiment and theory for cyclohexanone are unlikely due to the anharmonic effect on ZPE. A possible explanation is that the ring structure of cyclohexanone can introduce stronger couplings among the normal modes and between the vibration and rotation motions, as compared to the linear structures. Until the underlying mechanisms for this discrepancy are understood, the calibration presented here should be applied only to simple straight and branched carbon chains.

In addition, when applying this calibration to molecules with functional groups other than ketones, one might expect that systematic errors could arise since electrostatic interactions with water molecules change substantially from hydrocarbons (dispersion forces) to alcohols and carboxylic acids (hydrogen bonding). Nevertheless, our calibration curve is derived from ketones that are more polar than alkanes but less polar than alcohols and carboxylic acids, which should help to mitigate such problems. Also, most sedimentary organic molecules of interest are long aliphatic chains with at most one or two functional groups. For such molecules, even large uncertainties for the few H atoms surrounding the functional group would have only a slight impact on overall δ^2H values.

Finally, deviations from our calibration are likely to arise with decreasing molecular size, because other systematic errors, e.g., rotational correction and rotation–vibration coupling, cannot be safely ignored for small molecules. Hence we suggest the use of the calibration be restricted to molecules with five or more carbon atoms. Also, because the effect of anharmonicity, as well as many other systematic errors, changes systematically with temperature, use of this calibration for temperatures outside the calibration range (0–100 °C) should be approached with caution.

5. CONCLUSIONS

Equilibrium $^2H/^1H$ fractionations between H_α in linear ketones and water were measured at 25, 50 and 70 °C via isotope exchange experiments with uncertainties typically between 10‰ and 20‰. Results are in the ranges of −170‰ to −150‰, −130‰ to −110‰, and +30‰ to −30‰ for primary, secondary and tertiary H_α, respectively. Primary and secondary H_α exhibit a positive temperature dependence, while tertiary H_α exhibit a negative temperature dependence. Fractionations were also calculated using vibrational frequencies from ab initio calculations (B3LYP/6-311G**), with a standard deviation of 4–8‰ for structurally similar H_α in different molecules. Systematic errors in the calculations are likely dominated by the omission of anharmonicity, and largely cancel in the value of α_{eq} by taking the ratio of β factors. Consequently, experimental and theoretical α_{eq} values match very well in both magnitude and temperature dependence, yielding a linear but temperature-dependent calibration curve with slope $= 1.081 - 0.00376T$ and intercept $= 8.404 - 0.387T$, where T is temperature in degrees Celsius. Since the effect of anharmonicity is of the same size for C-bound H in most linear compounds other than ketones, we propose that this calibration can be applied to analogous theoretical calculations for a wide variety of organic molecules with linear carbon skeletons containing five or more C atoms, and for temperatures in the range of 0–100 °C. Considering all sources of uncertainty, we estimate that this approach should yield results that are accurate to within 10–20‰.

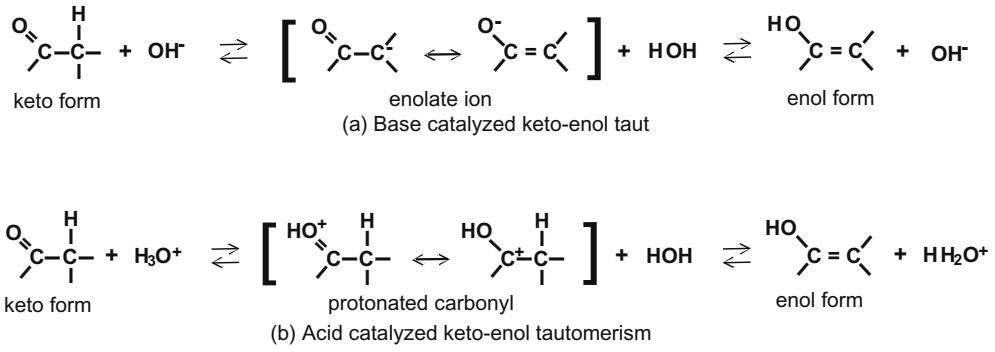

Fig. A1. Mechanisms of (a) base- and (b) acid- catalyzed H_α substitution.

ACKNOWLEDGMENTS

The authors thank Arndt Schimmelmann for the analysis of ^2H-enriched water standards employed here. We also acknowledge Adri van Duin, Edwin A. Schauble and Weifu Guo for helpful discussion on ab initio calculations. This work was supported by the Petroleum Research Fund (PRF) of the American Chemical Society (ACS), #43746-G2 and National Science Foundation (NSF) grant #EAR-0645502.

APPENDIX A. MECHANISM OF H_A SUBSTITUTION

H_α substitution in carbonyl compounds, including ketones, carboxylic acids, and the derivatives (R(C═O)X, $X = OH/O^-/OR/SR/NH_2\ldots$), takes place via keto-enol tautomerism that can be catalyzed by both base and acid conditions. In basic environment, H_α is abstracted by a base moiety to leave an enolate ion that is resonance-stabilized with the negative charge spread over the carbon and oxygen atoms (Fig. A1-a). Reprotonation by water molecules can occur either on C_α to regenerate the keto form or on the oxygen to produce the enol form. For simple ketones and aldehydes, the keto form predominates (99.99%). The rate-limiting step is deprotonation by hydroxide ion. Therefore the pseudo-first-order rate constant can be expressed as $k = k_{OH}\ [OH^-]$, where k_{OH} is the second-order rate constant. Acid-catalyzed exchange is initiated by protonating the oxygen, which further acidifies the H_α and thus allows water to abstract the proton (Fig. A1-b).

APPENDIX B. KINETICS OF H_A SUBSTITUTION

Isotope exchange reactions between an organic molecule and water can be described by the first-order rate equation (Roberts and Urey, 1939; Wedeking and Hayes, 1983):

$$\frac{F_t - F_e}{F_i - F_e} = e^{-kt}$$

where k is the pseudo-first-order rate constant and F_i, F_t and F_e are the fractional abundance of ^2H for the organic molecules *i*nitially, at time t, and at *e*quilibrium. At natural ^2H abundances, δ^2H values can be approximately substituted for F's (Roberts and Urey, 1939; Sessions et al., 2004). Therefore by regressing $\ln[(\delta^2H_t - \delta^2H_e)/(\delta^2H_i - \delta^2H_e)]$ versus time, the apparent first-order rate constant (k_{obsd}) can be obtained as the negative slope. For base-catalyzed H_α exchange, $k_{obsd} = k_{OH}\ [OH^-]$, where k_{OH} is the second-order rate constant (see Appendix A). Moveover, the substitution to give monodeuterated product proceeds p times faster than to exchange all the H_α atoms, where p is the number of equivalent H_α atoms in the molecule. Therefore the true value of k_{OH} is equal to $pk_{obsd}/[OH^-]$. Knowing k_{OH}, k_{obsd} can then be estimated at various pH values.

Activation energy was obtained according to the Arrhenius relationship,

$$k_{OH} = Ae^{-\frac{E_a}{RT}}$$

where E_a is the activation energy; T is temperature in Kelvin; R is the gas constant; A is a constant. By regressing the natural log of k_{OH} (measured at 25, 50 and 70 °C) versus reciprocal temperature, E_a can be calculated from the regression slope.

APPENDIX C. SUPPLEMENTARY DATA

Supplementary data associated with this article can be found, in the online version, at doi:10.1016/j.gca.2009.08.019.

REFERENCES

Alexander R., Kagi R. I. and Larcher A. V. (1982) Clay catalysis of aromatic hydrogen-exchange reactions. *Geochim. Cosmochim. Acta* **46**, 219–222.

Amyes T. L. and Richard J. P. (1996) Determination of the p*K*(a) of ethyl acetate: Bronsted correlation for deprotonation of a simple oxygen ester in aqueous solution. *J. Am. Chem. Soc.* **118**, 3129–3141.

Andersen N., Paul H. A., Bernasconi S. M., McKenzie J. A., Behrens A., Schaeffer P. and Albrecht P. (2001) Large and rapid climate variability during the Messinian salinity crisis: evidence from deuterium concentrations of individual biomarkers. *Geology* **29**, 799–802.

Becke A. D. (1993) Density-functional thermochemistry. 3. The role of exact exchange. *J. Chem. Phys.* **98**, 5648–5652.

Bigeleisen J. and Mayer M. G. (1947) Calculation of equilibrium constants for isotopic exchange reactions. *J. Chem. Phys.* **15**, 261–267.

Chikaraishi Y. and Naraoka H. (2003) Compound-specific delta D-delta C-13 analyses of *n*-alkanes extracted from terrestrial and aquatic plants. *Phytochemistry* **63**, 361–371.

Chikaraishi Y., Naraoka H. and Poulson S. R. (2004a) Carbon and hydrogen isotopic fractionation during lipid biosynthesis in a higher plant (*Cryptomeria japonica*). *Phytochemistry* **65**, 323–330.

Chikaraishi Y., Naraoka H. and Poulson S. R. (2004b) Hydrogen and carbon isotopic fractionations of lipid biosynthesis among terrestrial (C3, C4 and CAM) and aquatic plants. *Phytochemistry* **65**, 1369–1381.

Coplen T. B. (1988) Normalization of oxygen and hydrogen isotope data. *Chem. Geo.* **72**, 293–297.

Criss R. E. (1999) *Principles of Stable Isotope Distribution*. Oxford University Press, New York, pp. 71–76.

Dawson D., Grice K. and Alexander R. (2005) Effect of maturation on the indigenous δD signatures of individual hydrocarbons in sediments and crude oils from the perth basin (Western Australia). *Org. Geochem.* **36**, 95–104.

Dawson D., Grice K., Wang S. X., Alexander R. and Radke J. (2004) Stable hydrogen isotopic composition of hydrocarbons in torbanites (Late Carboniferous to Late Permian) deposited under various climatic conditions. *Org. Geochem.* **35**, 189–197.

Estep M. F. and Hoering T. C. (1981) Stable hydrogen isotope fractionations during autotrophic and mixotrophic growth of microalgae. *Plant Physiol.* **67**, 474–477.

Felipe M. A., Kubicki J. D. and Rye D. M. (2003) Hydrogen isotope exchange kinetics between H_2O and H_4SiO_4 from ab initio calculations. *Geochim. Cosmochim. Acta* **67**, 1259–1276.

Feng X. H. and Epstein S. (1994) Climatic implications of an 8000-year hydrogen isotope time-series from bristlecone-pine trees. *Science* **265**, 1079–1081.

Galimov E. M. (1971) Relation between isotope separation factor and equilibrium constants for carbon isotope exchange reactions in hydrocarbon systems. *Russ. J. Phys. Chem.* **45**, 665–667.

Gourier D., Robert F., Delpoux O., Binet L., Vezin H., Moissette A. and Derenne S. (2008) Extreme deuterium enrichment of organic radicals in the Orgueil meteorite: revisiting the interstellar interpretation? *Geochim. Cosmochim. Acta* **72**, 1914–1923.

Greeley B. H., Russo T. V., Mainz D. T., Friesner R. A., Langlois J. M., Goddard W. A., Donnelly R. E. and Ringnalda M. N. (1994) New pseudospectral algorithms for electronic-structure calculations — length scale separation and analytical 2-electron integral corrections. *J. Chem. Phys.* **101**, 4028–4041.

Hartshorn Sr. and Shiner V. J. (1972) Calculation of h/d, c-12/c-13, and c-12/c-14 fractionation factors from valence force fields derived for a series of simple organic-molecules. *J. Am. Chem. Soc.* **94**, 9002–9012.

Hill P. S. and Schauble E. A. (2008) Modeling the effects of bond environment on equilibrium iron isotope fractionation in ferric aquo–chloro complexes. *Geochim. Cosmochim. Acta* **72**, 1939–1958.

Horita J. and Wesolowski D. J. (1994) Liquid–vapor fractionation of oxygen and hydrogen isotopes of water from the freezing to the critical-temperature. *Geochim. Cosmochim. Acta* **58**, 3425–3437.

Huang Y. S., Wang Y., Alexandre M. R., Lee T., Rose-Petruck C., Fuller M. and Pizzarello S. (2005) Molecular and compound-specific isotopic characterization of monocarboxylic acids in carbonaceous meteorites. *Geochim. Cosmochim. Acta* **69**, 1073–1084.

Jancso G. and Van Hook W. A. (1974) Condensed phase isotope-effects (especially vapor–pressure isotope-effects). *Chem. Rev.* **74**, 689–750.

Knyazev D. A., Myasoedov N. F. and Bochkarev A. V. (1992) The theory of the equilibrium isotope effects of hydrogen. *Russ. Chem. Rev.* **61**, 204–220.

Koepp M. (1978) D/H isotope exchange reaction between petroleum and water: a contributory determinant for D/H-isotope ratios in crude oils? In *The Fourth International Conference, Geochronology, Cosmochronology, Isotope Geology USGS Open-File Report 78-701* (ed. R.E. Zartman). U.S. Geological Survey. pp. 221–222.

Krull E., Sachse D., Mugler I., Thiele A. and Gleixner G. (2006) Compound-specific delta C-13 and delta H-2 analyses of plant and soil organic matter: a preliminary assessment of the effects of vegetation change on ecosystem hydrology. *Soil Biol. Biochem.* **38**, 3211–3221.

Langley C. H., Lii J. H. and Allinger N. L. (2001) Molecular mechanics calculations on carbonyl compounds. II. Open-chain ketones. *J. Comput. Chem.* **22**, 1426–1450.

Larcher A. V., Alexander R., Rowland S. J. and Kagi R. I. (1986) Acid catalysis of alkyl hydrogen-exchange and configurational isomerization-reactions — acyclic isoprenoid acids. *Org. Geochem.* **10**, 1015–1021.

Lee C. T., Yang W. T. and Parr R. G. (1988) Development of the colle-salvetti correlation-energy formula into a functional of the electron-density. *Phys. Rev. B* **37**, 785–789.

Li C., Sessions A. L., Kinnaman F. S. and Valentine D. L. (2009) Hydrogen-isotopic variability in lipids from Santa Barbara Basin sediments. *Geochim. Cosmochim. Acta* **73**, 4803–4823.

Liu Y. and Tossell J. A. (2005) Ab initio molecular orbital calculations for boron isotope fractionations on boric acids and borates. *Geochim. Cosmochim. Acta* **69**, 3995–4006.

Lis G., Wassenaar L. I. and Hendry M. J. (2007) High-precision laser spectroscopy D/H and 18O/16O measurements of microliter natural water samples. *Anal. Chem.* **80**, 287–293.

Meloche H. P., Monti C. T. and Cleland W. W. (1977) Magnitude of the equilibrium isotope effect on carbontritium bond synthesis. *Biochim. Biophys. Acta Enzymol.* **480**, 517–519.

O'Neil J. R. (1986) Theoretical and experimental aspects of isotopic fractionation. In *Stable Isotopes in High Temperature Geological Processes 16* (eds. J.W. Valley, H.P. Taylor Jr., J.R. O'Neil). Am. Mineral. pp. 1–40.

Otake T., Lasaga A. C. and Ohmoto H. (2008) Ab initio calculations for equilibrium fractionations in multiple sulfur isotope systems. *Chem. Geo.* **249**, 357–376.

Pagani M., Pedentchouk N., Huber M., Sluijs A., Schouten S., Brinkhuis H., Damste J. S. S. and Dickens G. R. (2006) Arctic hydrology during global warming at the Palaeocene/Eocene thermal maximum. *Nature* **442**, 671–675.

Pedentchouk N., Freeman K. H. and Harris N. B. (2006) Different response of delta D values of *n*-alkanes, isoprenoids, and kerogen during thermal maturation. *Geochim. Cosmochim. Acta* **70**, 2063–2072.

Richard J. P., Williams G., O'Donoghue A. C. and Amyes T. L. (2002) Formation and stability of enolates of acetamide and acetate anion: an eigen plot for proton transfer at alpha-carbonyl carbon. *J. Am. Chem. Soc.* **124**, 2957–2968.

Richet P., Bottinga Y. and Javoy M. (1977) Review of hydrogen, carbon, nitrogen, oxygen, sulfur, and chlorine stable isotope fractionation among gaseous molecules. *Ann. Rev. Earth Planet. Sci.* **5**, 65–110.

Roberts I. and Urey H. C. (1939) Kinetics of the exchange of oxygen between benzoic acid and water. *J. Am. Chem. Soc.* **61**, 2580–2584.

Sachs J. P., Sachse D., Smittenberg R. H., Zhang Z., Battisti D. S. and Golubic S. (2009) Southward movement of the Pacific intertropical convergence zone AD 1400–1850. *Nat. Geosci.* **2**, 519–525.

Sauer P. E., Schimmelmann A., Sessions A. L. and Topalov K. (2009) Simplified batch equilibration for D/H determination of

non-exchangeable hydrogen in solid organic material. *Rapid Commun. Mass Spec.* **23**, 949–956.

Schimmelmann A. (1991) Determination of the concentration and stable isotopic composition of nonexchangeable hydrogen in organic-matter. *Anal. Chem.* **63**, 2456–2459.

Schimmelmann A. and Deniro M. J. (1993) Preparation of organic and water hydrogen for stable isotope analysis — effects due to reaction vessels and zinc reagent. *Anal. Chem.* **65**, 789–792.

Schimmelmann A., Lewan M. D. and Wintsch R. P. (1999) D/H isotope ratios of kerogen, bitumen, oil, and water in hydrous pyrolysis of source rocks containing kerogen types I, II, IIS, and III. *Geochim. Cosmochim. Acta* **63**, 3751–3766.

Schimmelmann A., Sessions A. L., Boreham C. J., Edwards D. S., Logan G. A. and Summons R. E. (2004) D/H ratios in terrestrially sourced petroleum systems. *Org. Geochem.* **35**, 1169–1195.

Schimmelmann A., Sessions A. L. and Mastalerz M. (2006) Hydrogen isotopic composition (D/H) of organic matter during diagenesis and thermal maturation. *Ann. Rev. Earth Planet. Sci.* **34**, 501–533.

Schoell M. and Whiticar M. J. (1982) Isotope geochemistry of natural gases in central-Europe. *J. Petrol. Geol.* **5**, 209–210.

Scott A. P. and Radom L. (1996) Harmonic vibrational frequencies: an evaluation of Hartree–Fock, Moller–Plesset, quadratic configuration interaction, density functional theory, and semi-empirical scale factors. *J. Chem. Phys.* **100**, 16502–16513.

Sessions A. L. and Hayes J. M. (2005) Calculation of hydrogen isotopic fractionations in biogeochemical systems. *Geochim. Cosmochim. Acta* **69**, 593–597.

Sessions A. L., Burgoyne T. W., Schimmelmann A. and Hayes J. M. (1999) Fractionation of hydrogen isotopes in lipid biosynthesis. *Org. Geochem.* **30**, 1193–1200.

Sessions A. L., Sylva S. P., Summons R. E. and Hayes J. M. (2004) Isotopic exchange of carbon-bound hydrogen over geologic timescales. *Geochim. Cosmochim. Acta* **68**, 1545–1559.

Stern M. J. and Wolfsberg M. (1966a) On absence of isotope effects in absence of force constant changes. *J. Chem. Phys.* **45**, 2618.

Stern M. J. and Wolfsberg M. (1966b) Simplified procedure for theoretical calculation of isotope effects involving large molecules. *J. Chem. Phys.* **45**, 4105.

Sternberg L., Deniro M. J. and Ajie H. (1984) Stable hydrogen isotope ratios of saponifiable lipids and cellulose nitrate from cam, C-3 and C-4 plants. *Phytochemistry* **23**, 2475–2477.

Tannor D. J., Marten B., Murphy R., Friesner R. A., Sitkoff D., Nicholls A., Ringnalda M., Goddard W. A. and Honig B. (1994) Accurate first principles calculation of molecular charge-distributions and solvation energies from ab-initio quantum-mechanics and continuum dielectric theory. *J. Am. Chem. Soc.* **116**, 11875–11882.

Thomson J. F. (1960) Fumarase activity in D_2O. *Arch. Biochem. Biophys.* **90**, 1–6.

Urey H. C. (1947) The thermodynamic properties of isotopic substances. *J. Chem. Soc.*(May), 562–581.

Urey H. C. and Rittenberg D. (1933) Some thermodynamic properties of the (HH2)-H-1, (HH2)-H-2 molecules and compounds containing the H-2 atom. *J. Chem. Phys.* **1**, 137–143.

Urey H. C., Brickwedde F. G. and Murphy G. M. (1932) A hydrogen isotope of mass 2. *Phys. Rev.* **39**, 164–165.

Van Hook W. A. (1968) Vapor pressures of isotopic waters and ices. *J. Phys. Chem.* **72**, 1234.

Wang Y. and Huang Y. S. (2001) Hydrogen isotope fractionation of low molecular weight *n*-alkanes during progressive vaporization. *Org. Geochem.* **32**, 991–998.

Wang Y. and Sessions A. L. (2008) Memory effects in compound-specific D/H analysis by gas chromatography/pyrolysis/isotope-ratio mass spectrometry. *Anal. Chem.* **80**, 9162–9170.

Wang Y., Sessions A. L., Nielsen R. J. and Goddard W. A. (2009) Equilibrium $^2H/^1H$ fractionations in organic molecules. Part II: Linear alkanes, alkenes, ketones, carboxylic acids, esters, alcohols and ethers. *Geochim. Cosmochim. Acta* **73**, 7076–7086.

Wedeking K. W. and Hayes J. M. (1983) Exchange of oxygen isotopes between water and organic material. *Isotope Geosci.* **1**, 357–370.

Whiticar M. J., Faber E. and Schoell M. (1985) Hydrogen and carbon isotopes of c-1 to c-5 alkanes in natural gases. *AAPG Bull.* **69**, 316 (abstr.).

Xu X. J., Xiao H. M., Gong X. D., Ju X. H. and Chen Z. X. (2005) Theoretical studies on the vibrational spectra, thermodynamic properties, detonation properties, and pyrolysis mechanisms for polynitroadamantanes. *J. Phys. Chem. A* **109**, 11268–11274.

Yang H. and Huang Y. S. (2003) Preservation of lipid hydrogen isotope ratios in Miocene lacustrine sediments and plant fossils at Clarkia, northern Idaho, USA. *Org. Geochem.* **34**, 413–423.

Young D. C. (2001) *Computational Chemistry: A Practical Guide for Applying Techniques to Real World Problems*. Wiley-Interscience, New York, pp. 92–98.

Zhang Z. and Sachs J. P. (2007) Hydrogen isotope fractionation in freshwater algae: I. Variations among lipids and species. *Org. Geochem.* **38**, 582–608.

Zhang X., Gillespie A. L. and Sessions A. L. (2009) Large D/H variations in bacterial lipids reflect central metabolic pathways. *Proc. Natl. Acad. Sci. USA* **106**, 12580–12586.

Associate editor: James Kubicki